analytical chemistry

Article

pubs.acs.org/ac

Simultaneous Determination of Reactive Oxygen and Nitrogen Species in Mitochondrial Compartments of Apoptotic HepG2 Cells and PC12 Cells Based On Microchip Electrophoresis–Laser-Induced Fluorescence

Zhenzhen Chen,[†] Qingling Li,[†] Qianqian Sun,[†] Hao Chen,[‡] Xu Wang,[†] Na Li,[†] Miao Yin,[†] Yanxia Xie,[†] Hongmin Li,[†] and Bo Tang*[,†]

[†]College of Chemistry, Chemical Engineering and Materials Science, Key Laboratory of Molecular and Nano Probes, Ministry of Education, Engineering Research Center of Pesticide and Medicine Intermediate Clean Production, Ministry of Education, Shandong Normal University, Jinan 250014, People's Republic of China

[‡]Center for Intelligent Chemical Instrumentation, Department of Chemistry and Biochemistry, Ohio University, Athens, Ohio 45701, United States

Supporting Information

ABSTRACT: Determination of intracellular bioactive species will afford beneficial information related to cell metabolism, signal transduction, cell function, and disease treatment. In this study, the first application of a microchip electrophoresis–laser-induced fluorescence (MCE–LIF) method for concurrent determination of reactive oxygen species (ROS) and reactive nitrogen species (RNS), i.e., superoxide ($O_2^{-\bullet}$) and nitric oxide (NO) in mitochondria, was developed using fluorescent probes 2-chloro-1,3-dibenzothiazolinecyclohexene (DBZTC) and 3-amino,4-aminomethyl-2′,7′-difluorescein (DAF-FM), respectively. Potential interference of intracellular dehydroascorbic acid (DHA) and ascorbic acid (AA) for NO detection with DAF-FM was eliminated through oxidation of AA with the addition of ascorbate oxidase, followed by subsequent MCE separation. Fluorescent products of $O_2^{-\bullet}$ and NO, DBZTC oxide (DBO), and DAF-FM triazole (DAF-FMT) showed excellent baseline separation within 1 min with a running buffer of 40 mM Tris solution (pH 7.4) and a separating electric field of 500 V/cm. The levels of DBO and DAF-FMT in mitochondria isolated from normal HepG2 cells and PC12 cells were evaluated using this method. Furthermore, the changes of DBO and DAF-FMT levels in mitochondria isolated from apoptotic HepG2 cells and PC12 cells could also be detected. The current approach was proved to be simple, fast, reproducible, and efficient. Measurement of the two species with the method will be beneficial to understand ROS/RNS distinctive functions. In addition, it will provide new insights into the role that both species play in biological systems.

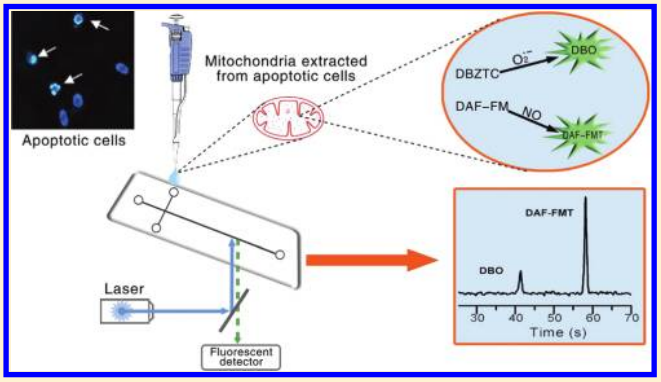

Reactive oxygen species (ROS), such as superoxide ($O_2^{-\bullet}$) and hydrogen peroxide (H_2O_2), and reactive nitrogen species (RNS), such as nitric oxide (NO) and peroxynitrite ($ONOO^-$), are important players in a multitude of pathophysiological conditions.[1] They have apparently dichotomous effects under certain circumstances. Appropriate amount of these species is essential to the immune response and many physiological signal transduction pathways; however, when overproduced, their chemical reactivity can lead to toxicity and tissue injury.[2] In addition to their respective biological activities, it is also important to investigate ROS and RNS relationships in complex biological situations. For example, the interaction between signaling molecule NO (produced endogenously by the action of NO synthase, NOS) and $O_2^{-\bullet}$ within mitochondria is of pathological significance and is also a potential mechanism for the regulation of mitochondrial function.[3] On one hand, the inhibition of cytochrome *c* oxidase[4] situated on the inner membrane of mitochondria by NO leads to increased superoxide production by respiratory complexes I and III. The overproduced superoxide can be effectively converted to more oxidizing hydrogen peroxide (H_2O_2) by mitochondrial superoxide dismutase (SOD). On the other hand, superoxide can inactivate NO action at a nearly diffusion-controlled speed to form peroxynitrite ($ONOO^-$),[5] a strong oxidant that can react with a vast number of other biomolecules to cause cell damage. Considering the important implication mechanism of mitochondrial $O_2^{-\bullet}$ and NO,

Received: September 22, 2011
Accepted: May 2, 2012
Published: May 2, 2012

together with their interaction for biochemical regulation, it is of interest to examine the production of $O_2^{-\bullet}$ and NO in mitochondria simultaneously.

To date, $O_2^{-\bullet}$ and NO are often detected individually by various analytical techniques, such as electron spin resonance (ESR),[6] electrochemistry with microelectrodes,[7,8] chemiluminescence,[9,10] flow cytometry,[11,12] and fluorimetry,[13] which have been successfully applied to estimate the production of either species in biological systems. However, the data obtained from two different situations could not track the contents of these two species and their relationships at the same time point. A potent method for simultaneous analysis of the two species is still urgently needed. Microchip electrophoresis coupled with laser-induced fluorescence (MCE−LIF) detection is a powerful tool for simultaneous measurement of complex ingredients,[14] with many attractive benefits such as chip size reduction, reagent consumption reduction, and analysis time decrease, which can reduce overall cost. The combination of different functions on a single microchip is also beneficial to maintain a completely closed system with merits of automation, contamination, human intervention reduction, and error elimination. In addition, the high aggregation of the laser beam is fit for samples with limited volume, which can greatly enhance the detection sensitivity. Diversified bioactive species such as DNA,[15] protein,[16] virus,[17] ROS,[18,19] GSH,[20] etc. have been analyzed with the method. From the perspective of technology, it is feasible to detect mitochondrial $O_2^{-\bullet}$ and NO concurrently.

Recently, we have successfully established $O_2^{-\bullet}$ and H_2O_2,[21] H_2O_2 and GSH[22] simultaneous determination platforms using the MCE−LIF method associated with ideal fluorescent probes and realized concomitant measurement of them in cell extracts and subcellular compartments. Undoubtedly, mutual interplay of bioactive species has become an area of intense research for the function of them in intricate biological processes.[23] As for cellular $O_2^{-\bullet}$ and H_2O_2, the short lifetime of $O_2^{-\bullet}$ will result in its transformation toward H_2O_2 and subsequent H_2O_2 accumulation; therefore, concurrent determination of them is significant for understanding their roles in cellular signal transduction.[21] During apoptosis, mitochondrial GSH concentration decreases while H_2O_2 concentration increases, reflecting the varying redox conditions in mitochondria; simultaneous detection of H_2O_2 and GSH during the apoptotic course may help further comprehend the apoptosis mechanism of different cell types.[22] $O_2^{-\bullet}$ and NO belong to different bioactive species, but their biological activities could be cancelled out by forming peroxynitrite. Due to the prompt conversion of $O_2^{-\bullet}$, the existence of mitochondrial nitric oxide synthase (mtNOS), and other biological activities associated with them, the levels of $O_2^{-\bullet}$ and NO in mitochondria during different pathophysiological conditions are difficult to predict, especially during apoptosis. It is well-known that the concentration range of bioactive species is a key determinant of their biological functions.[24,25] Therefore, concurrent measurement of both species is important for understanding their precise roles in related research.

Herein, we have developed an MCE−LIF method for simultaneous analysis of superoxide and nitric oxide using fluorescent probes of 2-chloro-1,3-dibenzothiazolinecyclohexene (DBZTC)[26] and 3-amino,4-aminomethyl-2′,7′-difluorescein (DAF-FM).[27,28] Interference from dehydroascorbic acid (DHA) and ascorbic acid (AA)[27] for DAF-FM usage was eliminated by a specific enzymatic reaction[28] and then separation of various derivative products to complete NO determination.[29] The optimum conditions including buffer type, concentration, and separating electric field intensity were determined. Using the MCE−LIF assay, we determined mitochondrial $O_2^{-\bullet}$ and NO in HepG2 cells and PC12 cells. We then attempted to monitor the changes of $O_2^{-\bullet}$ and NO levels in mitochondria during cell apoptosis, since it is suggested that the mitochondria plays a central role in response to cell survival, while mitochondrial $O_2^{-\bullet}$ and NO are recognized as important regulators of apoptotic pathways.[30] To induce cell apoptosis, resveratrol that exerts antiproliferative and apoptotic actions on cancer cell lines, and amyloid β (Aβ) that is a major factor in the pathogenesis of Alzheimer's disease (AD), were introduced to HepG2 cells and PC12 cells, respectively. The method characteristics, time course change of mitochondrial DBO and DAF-FMT levels of the two cell types during apoptosis were studied. The results confirmed the feasibility of the method, which provided new chances for understanding both species' pathobiological and therapeutic basis for diverse diseases.

EXPERIMENTAL SECTION

Reagents. All chemicals and solvents used were of analytical grade. Water was purified with a Sartorius Arium 611 VF system (Sartorius AG, Germany) to a resistivity of 18.2 MΩ·cm. DBZTC was synthesized in our laboratory. 3-Amino,4-aminomethyl-2′,7′-difluorescein, diacetate (DAF-FM DA) and diethylamine NONOate (DEANO) were obtained from Sigma-Aldrich Chemicals (St. Louis, MO, U.S.A.). Stock solutions of DBZTC and DAF-FM DA (5.0 mM) were prepared in dimethyl sulfoxide (DMSO) and stored at −20 °C in darkness separately. For further use, the working solutions of DBZTC and DAF-FM DA were prepared by diluting the stock solutions. The preparation and purification of DBZTC oxide (DBO) followed the procedure from ref 26. Its stock solution was prepared by dissolving DBO in DMSO to 1 mM. Tris, borate, HEPES, and phosphate buffer used for electrophoretic migration were prepared by dissolving appropriate amount of Tris, $Na_2B_4O_7$, HEPES, and NaH_2PO_4 in ultrapure water, respectively. The required pH was adjusted by adding the appropriate amount of HCl or NaOH. Ascorbate oxidase from *Cucurbita* sp. (AO, lyophilized powder, Sigma) was dissolved in 100 mM PBS (containing 0.5 mM EDTA, pH 5.6) before use. Due to the instability of dehydroascorbic acid (DHA), its solution was freshly made in a nitrogen-purged buffer before use.

For cell treatment, a 5.0 mM resveratrol (Sigma) was prepared in DMSO. Subsequent dilutions were done in culture medium. Amyloid β_{25-35} peptide (Aβ_{25-35}, Sigma) was dissolved at 2 mM in sterile deionized water and kept frozen until use. The peptide was incubated at 37 °C for 2 days to prepare aggregated Aβ_{25-35} fibrils.[31] The solution was then diluted to the required concentration with serum-free DMEM. Aβ_{25-35} was used at 30 μM in all procedures unless otherwise stated.

DAF-FM and DAF-FMT Solution Preparation. DAF-FM DA is a cell-permeable fluorescent probe for the detection of nitric oxide intracellularly, which is hydrolyzed to DAF-FM by intracellular esterases. As for nitric oxide quantification and mitochondrial determination, DAF-FM was prepared just before use by adding the appropriate amount of esterase (Sigma) to the desired concentration of DAF-FM DA solution.

dx.doi.org/10.1021/ac300255n | Anal. Chem. 2012, 84, 4687−4694

A NO donor, DEANO, produces two molecules of NO each.[32] The delivery of NO can easily be controlled by preparing moderately basic solutions of the NONOate and then lowering the pH to initiate NO generation. Stock solution of NO (12.9 mM) was prepared by dissolving 1.0 mg of crystalline DEANO in 1 mL of 0.01 M sodium hydroxide solution. Working solutions were prepared by dilution of the alkaline NONOate solution in 0.1 M deoxygenated phosphate buffer (pH 7.4).

Standard solutions of DAF-FMT were obtained by combining different concentrations of NO solutions with 2 μM DAF-FM; then the mixed solutions were allowed to react for 40 min at 37 °C.

Cell Culture and Treatment. HepG2 cells (American Type Culture Collection, Manassas, VA) were grown in cell culture media and incubated at 37 °C in a humidified atmosphere of 5% CO_2 and 95% air. The cell culture medium was RPMI-1640 (Hyclone, U.S.A.) supplemented with 10% newborn calf serum (Gibco, Invitrogen), 1% penicillin, and 1% streptomycin.

PC12 cells, obtained from the Chinese Type Culture Collection (Shanghai Institute of Cell Biology, Chinese Academy of Science, China), were grown in cell culture media and incubated at 37 °C in a humidified atmosphere of 5% CO_2 and 95% air. The cell culture medium was high-glucose DMEM (Hyclone, U.S.A.) supplemented with 10% newborn calf serum (Gibco, Invitrogen), 1% penicillin, and 1% streptomycin. Cell viability was determined by the trypan-blue exclusion assay.

When cells were in a logarithmic growth phase, resveratrol at a final concentration of 100 μM was administered into the HepG2 cell culture medium. As for the Aβ_{25-35}-induced apoptosis, a final concentration of 30 μM was administered into the PC12 cell.

Preparation of Mitochondrial Extracts. Before and after treatment of cells with apoptosis-inducing reagent, mitochondria were prepared by differential centrifugation using a commercially available Beyotime mitochondria isolation kit (Beyotime Inst. Biotech, Haimen, China) with the aid of a dounce homogenizer. After centrifugation (Sigma, 3K15, Germany), the mitochondria pellet was suspended in uptake buffer (70 mM sucrose, 1 mM KH_2PO_4, 5 mM sodium succinate, 5 mM HEPES, 220 mM mannitol, 0.1 mM EDTA, pH 7.4) to a final concentration of 0.5 mg/mL protein. All steps were performed below 4 °C, and the isolated mitochondrial sample was kept on ice until being used in the experiments.

Mitochondria Treatments. For superoxide depletion, Tiron, an SOD mimetic that scavenges superoxide, was added into the mitochondria extract to a final concentration of 1 mM. Depletion of nitric oxide was performed by addition of 10 μM hemoglobin to the mitochondrial extract. When needed, the mitochondrial extracts were treated with 5 μM rotenone to inhibit mitochondiral respiration. Then the mitochondrial solutions were determined according to the microfluidic electrophoresis procedure.

Protein Quantification. To measure the protein concentration in a mitochondrial extract, the dye-binding assay of Bradford was used with Bradford protein assay kit (Beyotime Inst. Biotech, Haimen, China). Absorbance at 595 nm was measured with a microplate reader RT6000 (Rayto, American).

Microfluidic System. The schematic diagram of the experimental setup is shown in the Supporting Information, Figure S1. The microfluidic system consisted of a glass microchip, a laser-induced fluorescence detector (LIFD), a versatile programmable eight-path-electrode power supply (PEPS), a data acquisition, and a personal computer. The microchip with a cross design was made in house. The channel cross section was close to a rectangle structure (70 μm width ×25 μm depth). Four reservoirs were the same column structure with 3 mm diameter and 1.5 mm depth. The glass microchip assembly was mounted on the $X-Y-Z$ translational stage of the LIFD. The laser detection point lay 30 mm downstream from the cross, C, in the separation channel. The PEPS was used for sample injection and MCE separation. The connecting interface between the PEPS and the chip was realized by dipping the four Pt electrodes (0.5 mm) of the PEPS into the four reservoirs of the microfluidic chip, respectively.

The LIFD and PEPS were both made in house. A low-noise semiconductor double-pumped solid-state laser (MLLIII-473 nm/20 mW, Changchun Xinchanye Guangdianjishu Co. Ltd., China) was reflected using a dichroic splitter (Omega Optical Inc., Brattleboro, VT, U.S.A.) and focused by a 40× objective lens (Leica instrument Co. Ltd., Germany) into the separation channel. The emitted fluorescence was collected by the same objective and penetrated through the same dichroic splitter, a band-pass filter, a focusing lens, a 500 μm pinhole, a 525 ± 5 nm narrow band filter, and was finally detected by an R928 photomultiplier (PMT, Hamamatsu, Japan). Signal output of the PMT passing through the I/V converters (OPA128, BB Inc., U.S.A.) was sampled using a CT-22 data acquisition card (the sampling frequency, 20 Hz, Shanghai Qianpu Shuju Co. Ltd., China). The computer incorporated with a program was used to control the PEPS and data acquisition.

Microfluidic Electrophoresis Procedure. The microchannels were rinsed sequentially with 0.1 M NaOH and ultrapure water for 10 min, respectively, before being flushed with electrophoresis buffer for 5 min. Prior to the MCE separation, sample waste (SW), buffer (B), and buffer waste (BW) reservoirs were all filled with 10 μL of electrophoresis running buffer, and sample reservoir (S) was filled with 10 μL of sample solution. The electrokinetic pinched sample injection and zone electrophoresis separation were controlled by the voltage output of the PEPS for each reservoir. During the pinched injection, 400 V was applied to the reservoir S for 30 s, 280 and 600 V were applied to the reservoirs B and BW, respectively, while reservoir SW was grounded. Separation was performed by applying 2500 V to reservoir B, 1800 V to the reservoirs S and SW with reservoir BW grounded.

All solutions were filtered through a 0.22 μm nylon syringe filter before being added into the chip.

Analysis of Fluorescent Products in Mitochondria. Mitochondria in uptake buffer was diluted and incubated at 37 °C in the presence of ascorbate oxidase, 2 μM DAF-FM, and 5 μM DBZTC for 40 min. Then the mitochondrial solutions were diluted 20 times in electrophoresis running buffer and measured according to the microchip electrophoresis procedure.

Statistical Analysis. Data were expressed as the mean ± standard deviation. All experiments were repeated three times, and the data were calculated with Microsoft Excel. For significance testing, the Student's t test was used (a $p < 0.05$ is considered significant).

dx.doi.org/10.1021/ac300255n | Anal. Chem. 2012, 84, 4687−4694

RESULTS AND DISCUSSION

Microchip Electrophoretic Optimization. Because of the similar fluorescence properties of their reaction products, DBZTC and DAF-FM were employed as labeling reagents for $O_2^{-\bullet}$ and NO (Supporting Information, Figure S2), respectively. DBZTC which has been utilized to detect superoxide in cell extracts using MCE–LIF methods in our previous works,[21,33] reacts with $O_2^{-\bullet}$ in a 1:1 molar ratio and the derivatization efficiency is quantitative, but DAF-FM has been seldom used for NO determination in conjunction with MCE–LIF methods, owing to the AA and DHA interferences.[34] In order to achieve reliable determination for $O_2^{-\bullet}$ and NO, the experimental conditions were carefully optimized to obtain the best sensitivity and selectivity for the targeted analytes under study, especially those for NO.

As shown in Figure 1, DAF-FM, newly prepared from DAF-FM DA through hydrolyzation by esterase, exhibited low background signal (5 μM, Figure 1). When the concentration of DAF-FM was under 2 μM, no background fluorescent signal was observed (2 μM, Figure 1). Therefore, subsequent NO determination was performed with 2 μM newly prepared DAF-FM. On the other hand, interference with DAF-FM assisted intracellular NO measurements[28] by dehydroascorbic acid (DHA) and ascorbic acid (AA) could be reduced effectively through conversion of AA to DHA by addition of ascorbate oxidase (AO), and Scheme 1 illustrates the solution of eliminating interference of AA and DHA with NO detection.

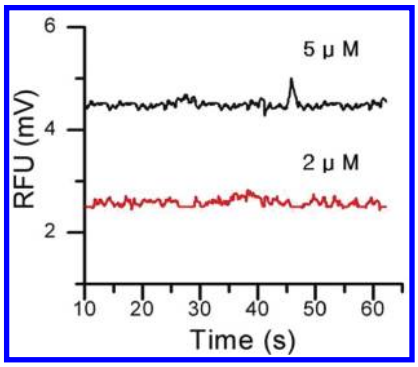

Figure 1. Typical microchip electropherograms of fluorescent probe of DAF-FM: bottom, 2 μM; top, 5 μM. Buffer: 50 mM Tris, pH 7.4.

Microchip electrophoresis separation of negatively charged DAF-FMT (fluorescent product of NO), DAF-FM-DHA (fluorescent product of DHA), and neutral DBO (fluorescent product of $O_2^{-\bullet}$ with DBZTC) was then investigated to achieve simultaneous determination of $O_2^{-\bullet}$ and NO. Four kinds of buffers (i.e., HEPES, phosphate, Tris, and borate buffers) were thus employed to gain better separation of DBO, DAF-FMT, and DAF-FM-DHA. Considering the potential application of the method for biological analysis, a suitable medium of pH 7.4 was selected, except that of borate buffer with pH 9.2. It was found that Tris buffer solution was the most suitable to obtain a compromise among a short analysis time, a higher column efficiency, and a better resolution (Supporting Information, Table S1).

The typical electrophoregram of DBO, DAF-FMT, and DAF-FM-DHA is illustrated in Figure 2, with DBO, DAF-FM-DHA, and DAF-FMT migration times of 41, 54, and 58 s under the optimized separation conditions, respectively. Separation can be completed within 1 min, indicating that simultaneous and rapid determination of $O_2^{-\bullet}$ and NO can be realized.

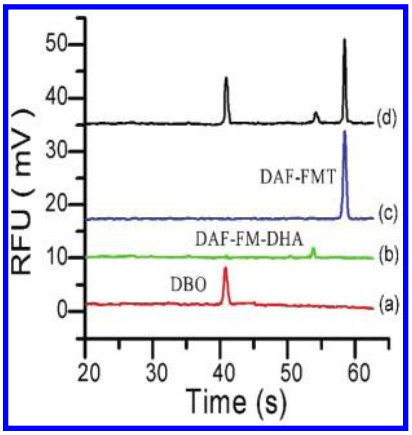

Figure 2. Electropherograms of standard solutions of fluorescent derivatives (from bottom to top): 100 nM DBO (a); DAF-FM-DHA (b); 50 nM DAF-FMT (c); DBO + DAF-FM-DHA + DAF-FMT (d). MCE conditions: running buffer, 40 mM Tris, pH 7.4; injection time, 30 s; separation electric field, 500 V/cm; effective separation distance, 30 mm.

Scheme 1. Eliminating AA/DHA Interference with NO Detection

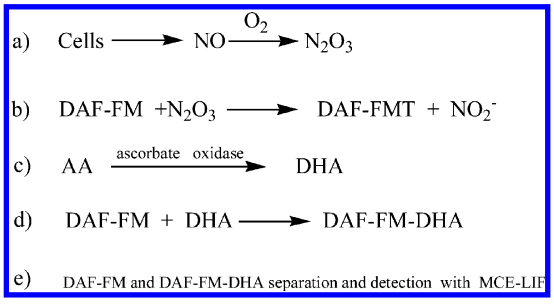

Analytical Characteristics of the Method. An investigation was performed to determine the linear range, limit of detection (LOD), and reproducibility, and the results are shown in Table 1. Under the optimized conditions, electrokinetic pinched sampling operations were used for injection and peak areas were used to acquire calibration lines. The calibration ranges obtained for DBO were 1.4×10^{-8} to 1.5×10^{-7} M and 1.5×10^{-7} to 1.5×10^{-6} M, and those obtained for DAF-FMT were 3.6×10^{-9} to 1.5×10^{-7} M and 1.5×10^{-7} to 5.0×10^{-6} M. The LODs, calculated based on signals equal to 3 times the standard deviation of the background, were 4.3 and 1.1 nM for DBO and DAF-FMT, respectively. The volume of the injected sample plug was experimentally measured to be 123 pL by visual checking using an inverted fluorescent microscope (DM-IL, Leica, Germany) and a charge-coupled device (CCD) camera (DFC300FX, Leica, Germany).[22] Therefore, the mass LODs for DBO and DAF-FMT were calculated to be 0.53 and 0.13 amol, respectively. Reproducibilities obtained from migration time and peak area measurements were studied by six injections of standard solutions of 100 nM DBO or 50 nM DAF-FMT consecutively.

Abundance of DBO and DAF-FMT in Mitochondria Isolated from HepG2 Cells. To assess the applicability of the proposed MCE–LIF detection assay for monitoring $O_2^{-\bullet}$ and NO simultaneously in real biological samples, the method was

dx.doi.org/10.1021/ac300255n | Anal. Chem. 2012, 84, 4687–4694

Table 1. Analytical Performance of the Proposed Method

analyte	regression equation[a]	R	linear range (M)	LOD (nM)[b]	RSD (%, n = 6) (migration time)	RSD (%, n = 6) (peak area)
DBO[c]	$y = (0.049 \pm 0.17) + (71.66 \pm 3.88)x$	0.9938	1.4×10^{-8}–1.5×10^{-7}	4.3	1.2	3.2
	$y = (2.86 \pm 1.43) + (44.20 \pm 0.99)x$	0.9972	1.5×10^{-7}–1.5×10^{-6}			
DAF-FMT[d]	$y = (0.11 \pm 0.27) + (270.91 \pm 8.44)x$	0.9980	3.6×10^{-9}–1.5×10^{-7}	1.1	1.8	4.1
	$y = (1.384 \pm 3.51) + (247.31 \pm 10.52)x$	0.9991	1.5×10^{-7}–5.0×10^{-6}			

[a] y, peak area (in mV·s); x, concentration of the analyte (in μM). [b] Concentration limits of detection measured for a signal/noise ratio of 3. The standard deviation of reagent blank is 0.103 (n = 10). [c] Species being detected: $O_2^{-\bullet}$. [d] Species being detected: NO.

first used to monitor the two species in mitochondria of HepG2 cells. The typical electropherogram is shown in Figure 3. On

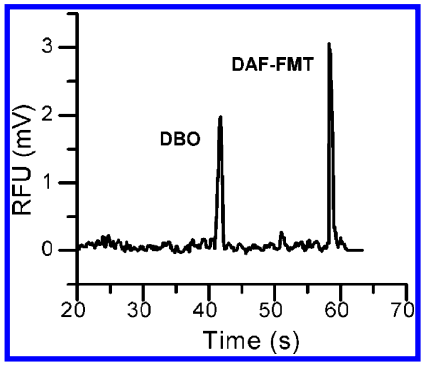

Figure 3. Typical microchip electropherogram of fluorescent products in mitochondria isolated from HepG2 cells. MCE conditions were the same as in Figure 2.

the basis of the migration times, the peaks corresponding to DBO and DAF-FMT were identified, which represented $O_2^{-\bullet}$ and NO, respectively. Although ascorbate oxidase was applied to eliminate the AA inhibition on DAF-FM and NO reaction, the signal of DAF-FM-DHA was almost negligible (Figure 3), probably because of more reactivity of DAF-FM to NO than to DHA[29] and because of the dilution of the mitochondrial samples during preparation. Ground on the linear regression equation and the peak area, the mitochondrial DBO and DAF-FMT contents were determined to be 0.84 ± 0.09 and 0.29 ± 0.04 μM (n = 3; mitochondrial protein concentration, 0.5 mg/mL), respectively.

The peak identification was further confirmed by depletion experiments, and the analytical results are illustrated in Figure 4. When Tiron was administered on mitochondria, the peak of DBO disappeared while the peak area of DAF-FMT increased slightly. Since $O_2^{-\bullet}$ can react with NO to form $ONOO^-$, reducing the $O_2^{-\bullet}$ concentration by Tiron can reduce $ONOO^-$ production and improve the bioavailability of NO under the circumstances. When hemoglobin was administered on mitochondria, the peak of DAF-FMT disappeared as expected, but the peak area of DBO remained almost unchanged. The reason for that might be due to the proportion of superoxide that is directed toward peroxynitrite formation in the system. If the majority of $O_2^{-\bullet}$ reacts with targets rather than NO, the production of $O_2^{-\bullet}$ will exceed that of NO. In this case, the added hemoglobin is likely to decrease $ONOO^-$ formation with no effect on $O_2^{-\bullet}$ production.[35]

Furthermore, nonrespiring mitochondria treated with rotenone were utilized as a control to confirm the biological significance of mitochondrial superoxide and nitric oxide

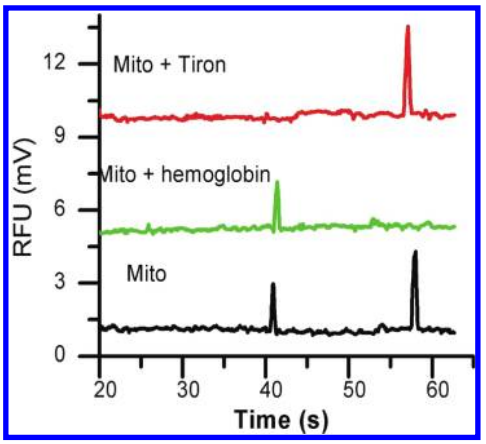

Figure 4. Typical microchip electropherogram of DBO and DAF-FMT in mitochondria isolated from HepG2 cells (black line); electropherogram of mitochondrial fluorescent products of HepG2 cells in the presence of hemoglobin (10 μM, green line) and Tiron (1 mM, red line). MCE conditions were the same as in Figure 2.

measurements by the proposed MCE–LIF method. Rotenone is a respiratory inhibitor that blocks electron transfer through complex I.[36] Upon addition of rotenone, the DBO peak area increased by ~2.7-fold (data not shown), a magnitude of change comparable with the 2–3-fold increment reported in literature,[37] indicating the superoxide release upon mitochondrial electron transfer block. Meanwhile, the DAF-FMT peak area had ~0.45-fold decrease (data not shown), with the possible reason that retonone could inactivate mitochondrial complex I, whereby complex I inactivation abolishes mtNOS activity, thus reducing the NO amount accordingly.[38]

Measurements of DBO and DAF-FMT in Isolated Mitochondria from HepG2 Cells Undergoing Apoptosis. The proposed MCE–LIF assay was next applied to survey variation of DBO and DAF-FMT levels in mitochondria during cell apoptosis. Resveratrol (trans-3,4′,5-trihydroxystilbene), a polyphenolic phytoalexin present mainly in grapes, red wine, and berries, was administrated on HepG2 cells to induce apoptosis. Resveratrol has been reported to have diverse beneficial actions, such as protecting cells and tissues against neurodegeneration, cardiovascular disease, cancer, and diabetes. Moreover, it is also known to possess strong chemopreventive and anticancer properties.[39] Herein, the antiproliferative and apoptosis-inducing activities of resveratrol in human HepG2 cells were investigated.

Studies indicated that resveratrol induced apoptosis in HepG2 cells in a dose- and time-dependent manner. A concentration of 100 μM resveratrol was administered on HepG2 cells according to the literature.[40] The DAPI staining for chromatin condensation assessment demonstrated a nuclear

dx.doi.org/10.1021/ac300255n | Anal. Chem. 2012, 84, 4687–4694

marginalization within 6 h after resveratrol treatment (Figure 5A) as an early sign of apoptosis. At the same time,

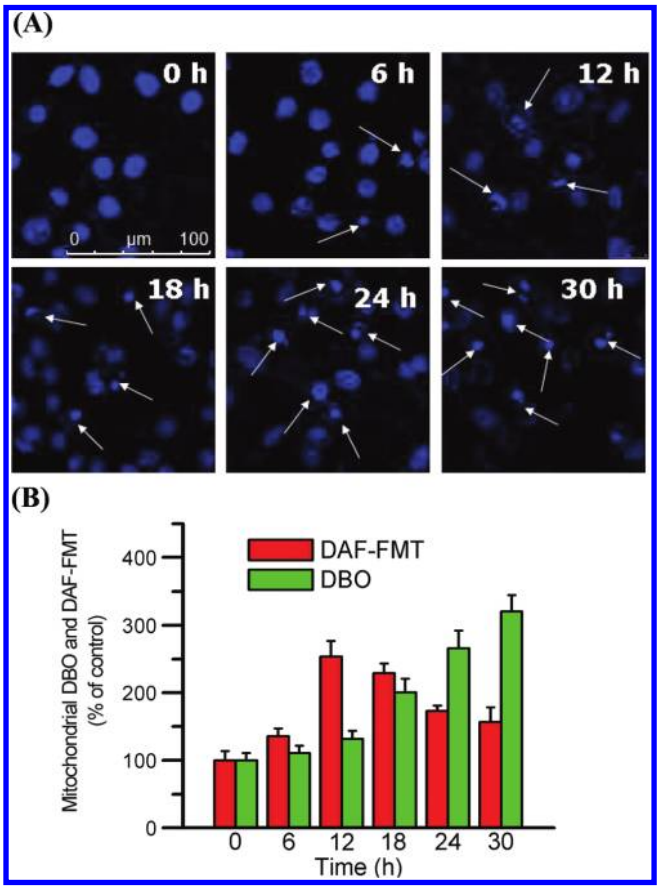

Figure 5. (A) DAPI staining of HepG2 cells upon 100 μM resveratrol treatment. (B) Time course of mitochondrial fluorescent product formation after resveratrol-induced HepG2 cell apoptosis. MCE conditions were the same as in Figure 2. Three independent measurements were carried out for each mitochondrial preparation. The error bar superimposed on each marker means SD.

mitochondrial DBO and DAF-FMT amounts all increased (Figure 5B), indicating that resveratrol-induced apoptosis involved the participation of $O_2^{-\bullet}$ and NO. It is interesting to note that the amounts of the two fluorescent products kept increasing and that of DAF-FMT reached a peak of almost 2.5 times versus control at 12 h of induction, partly because of resveratrol modulation of mitochondrial NOS expression and activation.[41] From then on, there is also an increase in the number of apoptotic cells, which were suggested by cell shrinkage, chromatin condensation, nuclear fragmentation, and shedding (Figure 5A), after treatment of cells with resveratrol for 18 and 24 h. The corresponding signal of DBO in mitochondria sustained a growing state and rose to 3 times until 30 h disposal with resveratrol; however, mitochondrial DAF-FMT amount decreased until resveratrol treatment for 30 h, suggesting that the activation of the NOS system might be only an early event of apoptosis[42] and the decrease in DAF-FMT might be due to NO reaction with $O_2^{-\bullet}$ to form more damaging $ONOO^-$.[5]

Measurements of DBO and DAF-FMT in Isolated Mitochondria from PC12 Cells Undergoing Apoptosis. Increasing evidence suggests an important role of mitochondrial dysfunction in the pathogenesis of Alzheimer's disease, the most common neurodegenerative disorder characterized by the presence of amyloid plaques and programmed cell death.[43,44] Thus, using the proposed MCE−LIF method, we investigated the effects of amyloidβ_{25-35} peptide (Aβ_{25-35}) on mitochondrial $O_2^{-\bullet}$ and NO production in PC12 cells, a useful in vitro model for neuronal differentiation. The typical electropherogram of untreated PC12 cells is shown in Figure 6, and the

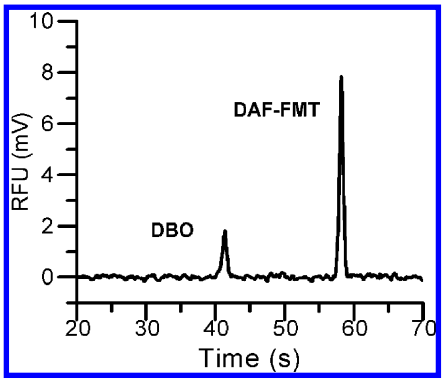

Figure 6. Typical microchip electropherogram of DBO and DAF-FMT in mitochondria isolated from PC12 cells. MCE conditions were the same as in Figure 2.

mitochondrial DBO and DAF-FMT contents were 0.70 ± 0.05 and 0.75 ± 0.11 μM (n = 3; mitochondrial protein concentration, 0.5 mg/mL), respectively. Excessive generation of DAF-FMT compared with liver cells manifested the important role of NO in signaling transduction in neuronal cells.[45]

It has been reported that Aβ can affect the dynamics of mitochondria, a process which involves the participation of ROS and NO.[46] Such a detailed work related to changes of mitochondrial $O_2^{-\bullet}$ and NO production has never been done before. Basal apoptosis of PC12 cells induced by 30 μM Aβ_{25-35} was then observed using DAPI staining. It was found that 6 h of incubation of PC12 cells with Aβ_{25-35} caused nuclear morphological change (Figure 7A) plus DBO and DAF-FMT amount increase (Figure 7B), suggesting that $O_2^{-\bullet}$ and NO may be mediators of Aβ_{25-35}-induced neuronal cell death. At 12 h, several cells lose chromatin integrity (Figure 7A) and both species keep increase to almost 2 times the level compared with control samples. After 18 h, the amount of DAF-FMT reached a platform and remained almost constant at 2.2 times in contrast to untreated mitochondria, but that of DBO showed sustained growth and featured a nearly 3.5-fold increase after 30 h of induction with Aβ (Figure 7B). Simultaneously, the DAPI staining demonstrated condensed chromatin gathering, nuclear fragmentation, and increased number of apoptotic cells, displaying the characteristics of apoptosis.

In short, mitochondria serve as an important cellular mediator of apoptosis, and different bioactive species such as ROS and RNS may participate in the process. Our experimental results implied that $O_2^{-\bullet}$ and NO were essential partners in the two cell types of apoptosis. Superoxide demonstrated unanimous increase, whereas nitric oxide showed a different trend during the process. This complexity may be a consequence of the rate of NO production and the interaction with other biological molecules such as $O_2^{-\bullet}$.

dx.doi.org/10.1021/ac300255n | Anal. Chem. 2012, 84, 4687−4694

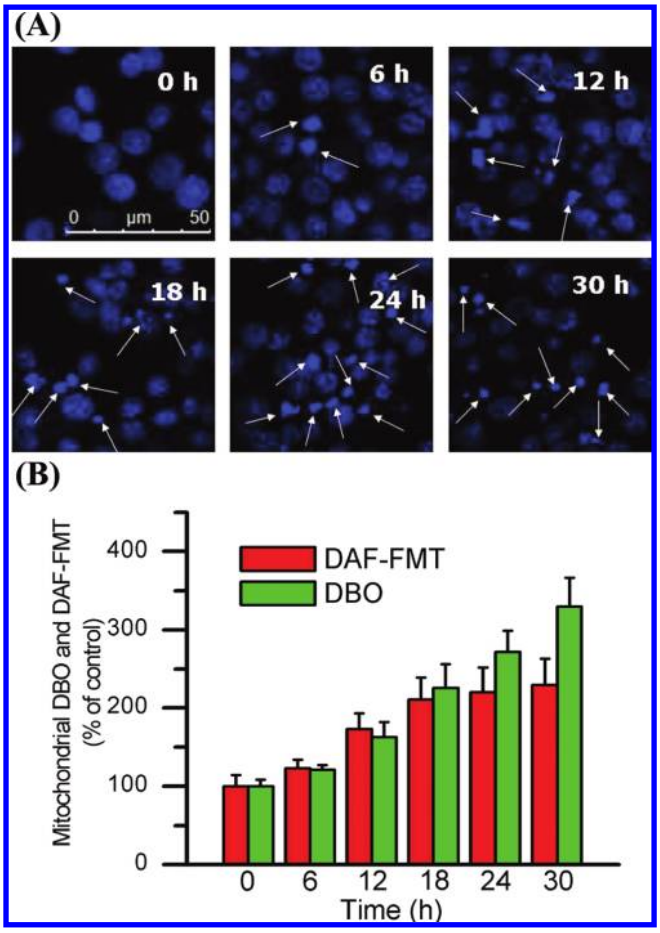

Figure 7. (A) DAPI staining of PC12 cells upon 30 μM Aβ_{25-35} treatment. (B) Time course of mitochondrial fluorescent products formation after Aβ_{25-35}-induced PC12 cell apoptosis. MCE conditions were the same as in Figure 2. Three independent measurements were carried out for each mitochondrial preparation. The error bar superimposed on each marker means SD.

CONCLUSION

In this work, the simultaneous determination of $O_2^{-\bullet}$ and NO using an MCE–LIF method has been established for the first time based on fluorescent probes DBZTC and DAF-FM. The feasibility of the assay was testified by measurement of the two ROS/RNS species in subcellular organelles. The tendency of the content change of the two species in mitochondria was obtained during the course of apoptosis. The method is simple, fast, reproducible, and efficient. Furthermore, it provides a powerful tool to study the functions and interactions of the two species and new chances for understanding their pathobiological and therapeutic basis for diverse diseases.

ASSOCIATED CONTENT

Supporting Information

Additional information as noted in text. This material is available free of charge via the Internet at http://pubs.acs.org.

AUTHOR INFORMATION

Corresponding Author

*E-mail: tangb@sdnu.edu.cn. Fax: 86-531-86180017.

Notes

The authors declare no competing financial interest.

ACKNOWLEDGMENTS

This work was supported by the National Key Natural Science Foundation of China (No. 21035003), the Specialized Research Fund for the Doctoral Program of Higher Education of China (20113704130001), the National Natural Science Foundation of China (No. 21105057), the Key Natural Science Foundation of Shandong Province of China (No. ZR2010BZ001), and the Program for Changjiang Scholars and Innovative Research Team in University. The first two authors contributed equally to this work.

REFERENCES

(1) West, A. P.; Brodsky, I. E.; Rahner, C.; Woo, D. K.; Erdjument-Bromage, H.; Tempst, P.; Walsh, M. C.; Choi, Y.; Shadel, G. S.; Ghosh, S. *Nature* **2011**, *472*, 476–480.
(2) Thomas, D. D.; Ridnour, L. A.; Isenberg, J. S.; Flores-Santana, W.; Switzer, C. H.; Donzelli, S.; Hussain, P.; Vecoli, C.; Paolocci, N.; Ambs, S.; Colton, C. A.; Harris, C. C.; Roberts, D. D.; Wink, D. A. *Free Radical Biol. Med.* **2008**, *45*, 18–31.
(3) Ghafourifar, P.; Schenk, U.; Klein, S. D.; Richter, C. *J. Biol. Chem.* **1999**, *274*, 31185–31188.
(4) Poderoso, J. J.; Lisdero, C.; Schopfer, F.; Riobo, N.; Carreras, M. C.; Cadenas, E.; Boveris, A. *J. Biol. Chem.* **1999**, *274*, 37709–37716.
(5) Moncada, S.; Erusalimsky, J. D. *Nat. Rev. Mol. Cell Biol.* **2002**, *3*, 214–220.
(6) Deschacht, M.; Horemans, T.; Martinet, W.; Bult, H.; Maes, L.; Cos, P. *Free Radical Res.* **2010**, *44*, 763–772.
(7) Amatore, C.; Arbault, S.; Bouton, C.; Drapier, J. C.; Ghandour, H.; Koh, A. C. *ChemBioChem* **2008**, *9*, 1472–1480.
(8) Wegerich, F.; Turano, P.; Allegrozzi, M.; Mohwald, H.; Lisdat, F. *Anal. Chem.* **2009**, *81*, 2976–2984.
(9) Yamaguchi, S.; Kishikawa, N.; Ohyama, K.; Ohba, Y.; Kohno, M.; Masuda, T.; Takadate, A.; Nakashima, K.; Kuroda, N. *Anal. Chim. Acta* **2010**, *665*, 74–78.
(10) Cornelius, J.; Tran, T.; Turner, N.; Piazza, A.; Mills, L.; Slack, R.; Hauser, S.; Alexander, J. S.; Grisham, M. B.; Feelisch, M.; Rodriguez, J. *Biol. Chem.* **2009**, *390*, 181–189.
(11) Mukhopadhyay, P.; Rajesh, M.; Batkai, S.; Kashiwaya, Y.; Hasko, G.; Liaudet, L.; Szabo, C.; Pacher, P. *Am. J. Physiol.: Heart Circ. Physiol.* **2009**, *296*, H1466–H1483.
(12) Carroll, J. S.; Ku, C. J.; Karunarathne, W.; Spence, D. M. *Anal. Chem.* **2007**, *79*, 5133–5138.
(13) Lebuffe, G.; Schumacker, P. T.; Shao, Z. H.; Anderson, T.; Iwase, H.; Vanden Hoek, T. L. *Am. J. Physiol.: Heart Circ. Physiol.* **2003**, *284*, H299–H308.
(14) Ling, Y. Y.; Yin, X. F.; Fang, Z. L. *Electrophoresis* **2005**, *26*, 4759–4766.
(15) Bliss, C. L.; McMullin, J. N.; Backhouse, C. J. *Lab Chip* **2007**, *7*, 1280–1287.
(16) Yang, W.; Sun, X.; Wang, H. Y.; Woolley, A. T. *Anal. Chem.* **2009**, *81*, 8230–8235.
(17) Reichmuth, D. S.; Wang, S. K.; Barrett, L. M.; Throckmorton, D. J.; Einfeld, W.; Singh, A. K. *Lab Chip* **2008**, *8*, 1319–1324.
(18) Qin, J.; Ye, N.; Yu, L.; Liu, D.; Fung, Y.; Wang, W.; Ma, X.; Lin, B. *Electrophoresis* **2005**, *26*, 1155–1162.
(19) Zhu, L.; Lu, M.; Yin, X. *Talanta* **2008**, *75*, 1227–1233.
(20) Gao, J.; Yin, X. F.; Fang, Z. L. *Lab Chip* **2004**, *4*, 47–52.
(21) Li, H.; Li, Q.; Wang, X.; Xu, K.; Chen, Z.; Gong, X.; Liu, X.; Tong, L.; Tang, B. *Anal. Chem.* **2009**, *81*, 2193–2198.
(22) Chen, Z.; Li, Q.; Wang, X.; Wang, Z.; Zhang, R.; Yin, M.; Yin, L.; Xu, K.; Tang, B. *Anal. Chem.* **2010**, *82*, 2006–2012.
(23) Brunati, A. M.; Pagano, M. A.; Bindoli, A.; Rigobello, M. P. *Free Radical Res.* **2010**, *44*, 363–378.
(24) Mishra, D. P.; Shaha, C. *J. Biol. Chem.* **2005**, *280*, 6181–6196.
(25) Burwell, L. S.; Brookes, P. S. *Antioxid. Redox Signaling* **2008**, *10*, 579–599.

(26) Gao, J. J.; Xu, K. H.; Tang, B.; Yin, L. L.; Yang, G. W.; An, L. G. *FEBS J.* **2007**, *274*, 1725−1733.
(27) Zhang, X.; Kim, W. S.; Hatcher, N.; Potgieter, K.; Moroz, L. L.; Gillette, R.; Sweedler, J. V. *J. Biol. Chem.* **2002**, *277*, 48472−48478.
(28) Kim, W. S.; Ye, X.; Rubakhin, S. S.; Sweedler, J. V. *Anal. Chem.* **2006**, *78*, 1859−1865.
(29) Ye, X.; Rubakhin, S. S.; Sweedler, J. V. *Analyst* **2008**, *133*, 423−433.
(30) Carreras, M. C.; Poderoso, J. J. *Am. J. Physiol.: Cell Physiol.* **2007**, *292*, C1569−C1580.
(31) Liu, X.; Feng, L.; Yan, M.; Xu, K.; Yu, Y.; Zheng, X. *Mol. Cell. Biochem.* **2010**, *344*, 277−284.
(32) Yang, Q.; Zhang, X.; Bao, X.; Lu, H.; Zhang, W.; Wu, W.; Miao, H.; Jiao, B. *J. Chromatogr., A* **2008**, *1201*, 120−127.
(33) Liu, X.; Li, Q.; Gong, X.; Li, H.; Chen, Z.; Tong, L.; Tang, B. *Electrophoresis* **2009**, *30*, 1077−1083.
(34) Nagata, N.; Momose, K.; Ishida, Y. *J. Biochem.* **1999**, *125*, 658−661.
(35) Manser, R. C.; Houghton, F. D. *J. Cell Sci.* **2006**, *119*, 2048−2055.
(36) Meany, D. L.; Thompson, L.; Arriaga, E. A. *Anal. Chem.* **2007**, *79*, 4588−4594.
(37) Xu, X.; Arriaga, E. A. *Anal. Chem.* **2010**, *82*, 6745−6750.
(38) Parihar, M. S.; Nazarewicz, R. R.; Kincaid, E.; Bringold, U.; Ghafourifar, P. *Biochem. Biophys. Res. Commun.* **2008**, *366*, 23−28.
(39) Notas, G.; Nifli, A. P.; Kampa, M.; Vercauteren, J.; Kouroumalis, E.; Castanas, E. *Biochim. Biophys. Acta* **2006**, *1760*, 1657−1666.
(40) Ma, X.; Tian, X.; Huang, X.; Yan, F.; Qiao, D. *Mol. Cell. Biochem.* **2007**, *302*, 99−109.
(41) Finocchietto, P. V.; Franco, M. C.; Holod, S.; Gonzalez, A. S.; Converso, D. P.; Antico Arciuch, V. G.; Serra, M. P.; Poderoso, J. J.; Carreras, M. C. *Exp. Biol. Med.(Maywood)* **2009**, *234*, 1020−1028.
(42) Hattori, R.; Otani, H.; Maulik, N.; Das, D. K. *Am. J. Physiol.: Heart Circ. Physiol.* **2002**, *282*, H1988−H1995.
(43) Keil, U.; Bonert, A.; Marques, C. A.; Scherping, I.; Weyermann, J.; Strosznajder, J. B.; Muller-Spahn, F.; Haass, C.; Czech, C.; Pradier, L.; Muller, W. E.; Eckert, A. *J. Biol. Chem.* **2004**, *279*, 50310−50320.
(44) Hardy, J.; Selkoe, D. J. *Science* **2002**, *297*, 353−356.
(45) Nisoli, E.; Carruba, M. O. *J. Cell Sci.* **2006**, *119*, 2855−2862.
(46) Kadowaki, H.; Nishitoh, H.; Urano, F.; Sadamitsu, C.; Matsuzawa, A.; Takeda, K.; Masutani, H.; Yodoi, J.; Urano, Y.; Nagano, T.; Ichijo, H. *Cell Death Differ.* **2005**, *12*, 19−24.